Mon. Not. R. Astron. Soc. **311**, 50–62 (2000)

The history of cosmic baryons: X-ray emission versus star formation rate

N. Menci[1] and A. Cavaliere[2]
[1]*Osservatorio Astronomico di Roma, via di Frascati 33, 00040 Monteporzio, Italy*
[2]*Astrofisica, Dipartimento Fisica, II Università di Roma, via Ricerca Scientifica 1, 00133 Roma, Italy*

Accepted 1999 August 2. Received 1999 July 2; in original form 1999 January 29

ABSTRACT

We relate the *star* formation from *cold* baryons condensing in virialized structures to the X-ray properties of the associated diffuse, *hot* baryonic component. Our computations use the standard 'semi-analytic' models to include and connect three sectors of the complex astrophysics involved: first, the formation of dark matter haloes through accretion and merging, after the standard hierarchical clustering; secondly, the star formation governed, after the current 'recipes', by radiative cooling and by feedback of the supernova energy into the hot baryonic component; thirdly, and novel, the hydrodynamics and thermodynamics of the hot phase, rendered with our Punctuated Equilibria model. So we relate the X-ray observables concerning the intracluster medium (namely, the luminosity–temperature relation, the luminosity functions, the source counts) to the thermal energy of the gas pre-heated and expelled by supernovae following star formation, and then accreted during the subsequent merging events.

Our main results are as follows. At fluxes fainter than $F_X \approx 10^{-15}\,\mathrm{erg\,cm^{-2}\,s^{-1}}$ the X-ray counts of extended extragalactic sources (as well as the faint end of the luminosity function, their contribution to the soft X-ray background, and the $L_X - T$ correlation at the group scales) increase considerably if the star formation rate is high for $z > 1$ as indicated by growing optical/infrared evidence. Specifically, the counts in the range 0.5–2 keV are increased by factors $\sim$4 when the the feedback is decreased and the star formation is enhanced as to yield a flat shape of the star formation rate for $2 < z < 4$.

Such faint fluxes are well within the reach of next generation X-ray observatories like *AXAF* and *XMM*. So very faint X-ray counts will soon constitute a new means of gaining information about the stellar processes (formation, and supernova feedback) at $z > 2$, and a new way to advance the understanding of the galaxy formation.

Key words: galaxies: clusters: general – galaxies: formation – intergalactic medium – X-rays: galaxies.

1 INTRODUCTION

The history and the fate of cosmic baryons constitute an open, outstanding problem in cosmology. It is matter of current debate their time-shifting partition among the stars and the diffuse cold and hot components, the latter being heated by stellar activity or at the expenses of the gravitational energy in the dark matter (DM) condensations.

Two lines of evidence enter the argument: one comes from the canonical bands, optical–ultaraviolet (O–UV) and infrared (IR); the other will come – we argue – from the X-ray band.

The first assessments from O–UV data of the global star formation rate (SFR) suggested a peak at $z \approx 1.5$ with a sharp decline out to $z \approx 4$ (Madau et al. 1996; Connolly et al. 1997); in such a picture, fewer than 20 per cent of the stars would have been formed at $z > 2$. Based on the hierarchical cold dark matter (CDM) models of structure formation, which predict the galaxy assembly to be a gradual process proceeding through merging and accretion events, such history has been modelled (see White & Frenk 1991; Cole et al. 1994; Kauffmann, White & Guiderdoni 1993; Baugh et al. 1998) by strongly coupling the star formation (SF) inside the haloes to their dynamical growth; in fact, the SFRs have been assumed to scale up considerably with the DM halo masses.

However, such a scenario has been seriously challenged by more recent observations (Pettini et al. 1997; Dickinson 1997; Meurer et al. 1997) indicating that the apparent decline for $z > 2$ was seriously affected by dust extinction; the underlying SFR may be increased by factors 3–15, up to yield a flat plateau for $z > 2$ (Madau, Pozzetti & Dickinson 1998). This picture is confirmed by the large statistics

obtained in denser fields by Steidel et al. (1998). Supporting independent evidence comes from the still scanty IR data obtained with SCUBA (see Smail, Ivison & Blain 1997; Hughes et al. 1998; Barger et al. 1999).

The issue, however, is still at stake. In fact, a flat SFR might easily lead to an overproduction of the IR background, and of the metal adundance in high-z absorbers (see Ellis 1998). Moreover, it is not clear how the optical fields sampled so far should be weighted to yield a reliable estimate of the average SFR.

Luckily, there is another angle to the baryon history. This is provided by the hot baryonic phase which is related to the SF and can be observed directly in X-rays as intracluster medium (ICM). A large amount of baryons corresponding to $\Omega_b/\Omega \approx 0.15$ is observed at $z \approx 0$ in galaxy groups and clusters on scales around $R \sim 1$ Mpc (White et al. 1993; White & Fabian 1995; see also Fukugita, Hogan & Peebles 1998). Such baryons are heated up to virial temperatures $kT \sim GMm_H/10R$ in the gravitational potential wells corresponding to masses $M \approx 10^{13}$–$10^{15}\,M_\odot$; at densities $n \approx 10^{-3}\,\mathrm{cm}^{-3}$ they emit by thermal bremsstrahlung copious X-rays with luminosities $L \propto R^3 n^2 T^{1/2} \approx 10^{44}\,\mathrm{erg\,s}^{-1}$. However, the ICM is not secluded; indeed, the shape of the $L_X - T$ correlation, which is observed to be bent from $L \propto T^2$ in very rich clusters (Allen & Fabian 1998) to a much steeper shape in groups (Ponman et al. 1996), indicates that the temperature of the external, infalling gas plays a key role in determining the X-ray properties of small groups and poor clusters (Cavaliere, Menci & Tozzi 1997, 1998, 1999; Balogh, Babul & Patton 1998). Such external temperature, in turn, may be set by supernova feedback to values exceeding the virial value in small merging lumps, so a connection is envisaged between the stellar processes and the astrophysics of the X-ray emitting ICM.

This connection will provide a relationship between the O, UV or IR observations and the X-ray data, which is the scope of this paper. In Cavaliere, Menci & Tozzi (1997, 1998a,b hereafter CMT97, CMT98, CMT99) we have already developed a semi-analytic approach to the X-ray emission, to deal with the DM merging histories, with the associated infall of external preheated gas, and with the resulting shock compression, all concurring to estabilish a sequence of approximate hydrostatic equilibria of the ICM (Punctuated Equilibria model). Our predicted, bent $L_X - T$ correlation is in excellent agreement with the observations; the parameter of the model is the initial temperature of external gas, which was assumed at a constant value around 0.5 keV adopted from simple estimates in the literature.

Such a temperature is of key importance as it happens to be close to the virial temperatures in typical groups, and may be surmised to rise gradually during structure formation. In addition, the amount of gas expelled by supernova feedback is essential in determining the amount of baryons filling of shallow potential wells, and hence the X-ray luminosity of small groups. So here we set out to compute these processes in full, based on the detailed recipes currently implemented in the semi-analytic models for star and galaxy formation (SAM hereafter, see Kauffmann, White & Guiderdoni 1993; Cole et al. 1994; Baugh et al. 1998; Somerville & Primack 1998) in hierachically evolving DM haloes. This allows us to connect in *one* framework the hierarchical clustering, the astrophysics of star-forming baryons, and the thermodynamics and hydrodynamics of the X-ray emitting plasma. In particular, we will show how forthcoming observations with *AXAF* and *XMM* can X-ray the SF history, so complementing the O–IR information.

2 THE MODEL

Towards our scope we need to relate both the SF and the astrophysics of the ICM to the gravitationally dominant DM content of the haloes. After the hierarchical clustering paradigm, the latter form as a result of the gravitational instability of initial random density fluctuations, and then evolve through stochastic merging of smaller or sometimes comparable units into larger structures. The resulting statistics is well estabilished in the form of the extended Press & Schechter theory (EPST, see Bond et al. 1991; White & Frenk 1991; Bower 1991; Lacey & Cole 1993).

As to the process of SF, we adopt an *analytic* rendition of the SAM approach. In the above papers the baryons gravitationally bound to a DM halo, after being heated to its virial temperature, are assumed to be exchanged among three phases: the *cold* phase produced by radiative cooling; the resulting *condensed* phase into stars; the *hot* phase constituted by gas preheated by supernova explosions and further raised to the virial temperature of the potential wells. The model includes coalescence of baryons following halo merging, and the luminosity–colour evolution owing to the rise and fall of successive star generations.

We include the X-ray emission in the very same framework, using the model proposed by CMT97: at each time-step the X-ray luminosity is computed from the hot phase of the ICM, and from the boundary conditions relating this to the external gas infalling in each merging event. As shown in CMT97–99, such boundary conditions are essential in providing a realistic model for the X-ray emission from clusters and groups. In fact, a set of equilibrium states exists for the ICM in a given halo, each corresponding to a different merging history and hence to a different boundary condition. The average X-ray luminosity corresponding to a given mass M is then obtained by convolving over all possible merging histories the emission corresponding to each equilibrium state.

Because of the added complexity to the standard SAMs, and of the related increase in computing time, we choose to express the merging histories analytically with the EPST rather than using the equivalent Monte Carlo simulations. Below we describe the basic ingredients of our model.

Whenever necessary, and until otherwise specified, the redshift z will be associated with the epoch t on adopting a critical universe with $H_0 = 50\,\mathrm{km\,s}^{-1}\,\mathrm{Mpc}^{-1}$.

2.1 Gas cooling, feedback and star formation rates

Our recipes to relate the SFR to the dynamics of DM haloes are basically taken from Cole et al. (1994) and are summarized as follows.

(a) For each DM mass M (or circular velocity $v_c \propto M^{1/3}$), the baryonic content is divided into a cold gas phase (able to radiatively cool within the halo) with mass m_c, into a star phase with mass m_*, and into the complementary hot phase with mass m_h. The initial gas content associated to all the haloes sums up to the universal baryonic density Ω_b. The initial stellar content at $z_i \sim 10$ is taken to be nil.

(b) The mass of the cold phase is increased from inside out by cooling processes; at each time-step Δt, we have then $\Delta m_c(v_c) = 4\pi r_{cool}^2 \rho_g \Delta r_{cool}$, where gas density ρ_g and the dependencies of the cooling radius r_{cool} on v_c and on t are given, e.g., by Somerville & Primack (1998). We adopt the cooling function used by Cole et al. (1994), which was computed assuming a primordial mixture of 77 per cent hydrogen and 23 per cent helium.

(c) Then it is computed the amount of cold gas which goes into stars, and the corresponding mass is transferred from the cold phase to the star phase. Such amount $\Delta m_*(v_c, t) = \dot{m}_* \Delta t$ is regulated by the SFR, namely $\dot{m}_*(v_c, t) = m_c/\tau_*$. The time-scale τ_* is parametrized in the form $\tau_*(v_c) = \tau_*^0 (v_c/300\,\mathrm{km\,s^{-1}})^{\alpha_*}$; the cold mass m_c is updated after each time-step by subtracting not only the mass of stars which have formed but also the cold gas expelled given below.

(d) A final transfer is due to supernova feedback from the cold back to the hot phase; this involves the amount $\Delta m_h = \beta(v_c)\Delta m_*(v_c, t)$, where the feedback per unit star mass is given by $\beta = (v_c/v_h)^{-\alpha_h}$, with the parameters v_h and α_h.

For each circular velocity v_c, we compute the further variations of the masses of the gas components and of the star content owing to merging of DM haloes (treated in detail in Section 2.3), possibly followed by galaxy coalescence. The latter is included on considering the probability that the galaxy coalescence time (parametrized as in Cole et al. 1994) is shorter than the halo survival time (depending on v_c), and by averaging over all possible halo merging histories (details are given in Poli et al. 1999). The values of the parameters τ_*^0, α_*, v_h and α_h are discussed in Section 3.

2.2 The X-ray emitting ICM

At the time t, the X-ray luminosity owing to bremsstrahlung emission by the hot baryons m_h in a halo of mass M is given by (CMT99)

$$L_X = A\left(\frac{m_h}{M}\right)^2 G^2(M, M')\; T_v^2(M)\; \rho^{1/2}\, I(M, t). \tag{1}$$

Here $T_v(M) = 4(M/10^{15}\,\mathrm{M_\odot})^{2/3}(1+z)\,\mathrm{keV}$ is the virial temperature corresponding to M; the average DM density inside the cluster is $\rho \propto (1+z)^3$; the normalization constant A will be adjusted so as to match the height of the observed local $L_X - T$ relation at $T = 4\,\mathrm{keV}$; the shape factor I describes the internal ICM distribution. Finally, G is the density jump (ratio) across the shock induced at the cluster boundary, at around the virial radius, by the infalling gas; this will depend not only on the cluster mass M, but also on the mass M' of the infalling clumps.

The contribution of emission lines has been included using the standard and public Raymond–Smith code.

We stress why the $L_X - T$ dependence differs from the self-similar power-law $L \propto T_v^2$. To a small degree this is due to the shape factor $I(M, t)$, a slowly varying function of M and t of the detailed form given by CMT99. This includes the integration over the cluster volume of the internal density run (normalized to the value at the virial radius); the latter is provided by the hydrostatic equilibrium once the gravitational potential $\phi(M)$ associated to M is given (we shall adopt the form given by Navarro, Frenk & White 1997).

Much more important is the strong dependence of G^2 on the halo merging histories; in fact, the (squared) compression ratio G^2 at the shock connects the ICM with the infalling gas associated with the merging partner of mass M'. Of this, the fraction f_* hovers around the clump M' having being expelled and heated to a temperature $T_*(M')$ by supernova feedback; the complementary fraction $1 - f_*$ is still contained inside the virial radius of M' at the virial temperature $T_v(M')$. During a merging event, both components fall into our well of mass M, and the compounded G^2 entering the luminosity (1) reads

$$G^2(M, M') = f_* g^2[T_*(M')] + (1 - f_*) g^2[T_v(M')]. \tag{2}$$

Here $g(T)$ denotes the shock compression factor for the inclusion of each gas fraction into a cluster or group, given in CMT98,99 to read

$$g(T) = 2\left(1 - \frac{T}{T_2}\right) + \left[\left(1 - \frac{T}{T_2}\right)^2 + \frac{T}{T_2}\right]^{1/2}; \tag{3}$$

the expression for T_2 is given by the same authors, and for strong shocks reads simply

$$kT_2(M) \approx \mu m_H \phi(M)/3 + 3kT/2,$$

where m_H is the proton mass. As anticipated above equation (2), the argument T in equation (3) takes one of the following two values: either the virial temperature (with the coefficient given by Metzler & Evrard 1997)

$$T_v(M') = 4(M'/10^{15}\,\mathrm{M_\odot})^{2/3}(1+z)\,\mathrm{keV} \tag{4}$$

for the $1 - f_*$ baryons retained in the lump M'; or the temperature of the ejected baryons provided (in the time-step Δt) by supernova feedback.

$$kT_*(M') = \frac{m_H}{3\Delta m_h} E_{SN}\,\eta_{SN}\,\dot{m}_*\Delta t = \frac{m_H}{3} E_{SN}\,\eta_{SN}\left(\frac{v_h}{v_c}\right)^{\alpha_h}, \tag{5}$$

where $E_{SN} = 10^{51}$ erg s^{-1} is the energy per supernova, η_{SN} is the number of supernovae per solar mass (3.2×10^{-3} for the Scalo IMF we shall use here); the latter equality holds after point (d) in Section 2.1. Note that the ratio $\dot{m}_* \Delta t / \Delta m_h = (v_h / v_c)^{\alpha_h}$ depends only on the current circular velocity of the halo and not on the progenitor masses.

Finally, the cold gas fraction f_* expelled outside the virial radius of M' and heated at $T_*(M')$ is computed adopting the Cole et al. (1994) recipe, i.e., assuming that the reheated gas is expelled from the halo. So the fraction of gas reheated in the time-step Δt reads

$$\Delta f_* = \Delta m_h / m_h. \tag{6}$$

Note that the quantity Δf_* depends on the merging history of the halo, as will be described in detail in Section 2.3.

Our guideline will be that, since the X-ray luminosity in equation (1) depends strongly on f_* and T_* which in turn depend on the star formation and on the feedback, a strong *correlation* must exist between the X-ray emission and the SFR.

2.3 Convolutions over the merging histories

Both the SF and the X-ray emission depend ultimately on the merging history of the haloes. In fact, at each merging event the gas reservoirs of a halo are increased by the gas (cold and hot) enclosed in the merging partner, and this changes the processes of cooling, feedback and SF together; in addition, by the sequence of overlapping merging events, the infalling gas compresses the ICM at the cluster boundary, and sets the X-ray luminosity (equation 1) through the factor G^2.

So to obtain the observable quantities – average value and scatter – associated to a halo, we must convolve over all merging histories leading to that mass. In detail, we adopt the following procedure, essentially an analytic rendition of the SAM, but complemented with the proper description of the physics of the X-ray emitting ICM.

(i) We define a time–velocity grid, with grid size $\Delta t = t_0/100$ and $\Delta v_c = 10\,\mathrm{km\,s^{-1}}$ (t_0 is the present cosmic time).

The number density $N(M, z_i)$ of DM haloes with mass M [or with circular velocity $v_c = (10\,G\,H(z)\,M)^{1/3}$] at the initial redshift $z_i \sim 10$ is taken from the Press & Schechter (1974) expression. Initially, to each halo we associate a galaxy with the same v_c of the halo (more than one galaxy per halo is an exceedingly rare circumstance for $z_i \sim 10$). For each v_c the corresponding mass M and virial temperature T_v are computed. As said above, the initial gas content associated to all haloes corresponds to the universal baryonic density Ω_b, and the initial stellar content is taken to be nil.

For each circular velocity v_c, the baryonic content is divided into *stars*, *cold* gas and *hot* gas as described in Section 2.1 under point (a).

(ii) At the next time-step, we compute the mass transfers: hot → cold → stars → hot, as described in Section 2.1, points (b), (c) and (d).

(iii) For each circular velocity v_c, we compute the further variations of the mass of the gas components and of the stars content owing to merging of DM haloes, possibly followed by galaxy coalescence. We also compute the compression factor G^2 (equation 2) and the corresponding X-ray luminosity (equation 1).

Since the merging process is stochastic, at each time-step and for each v_c (corresponding to M) we compute the probability density $\partial^2 P(M', t|M,)/\partial M' \partial t$ that a halo of mass M' has merged with a halo of complementary mass $M - M'$, to yield the considered M in the time interval Δt; within the standard hierarchical clustering, such a probability is provided by the EPST.

The average mass of the cold and the hot gas contents in a halo with circular velocity v_c are updated according to following equation, analogous to White & Frenk's (1991):

$$m_h(v_c, t + \Delta t) = m_h(v_c, t) + \Delta t \int_0^{M(v_c)} \mathrm{d}M' \frac{N(M', t)}{N(M, t)} \frac{\partial^2 P(M', t|M)}{\partial M' \partial t} m_h(M'). \tag{7}$$

This yields the average increment due to the merging, together with the haloes, of previous baryon reservoirs. An analogous equation holds for the baryonic mass in stars $m_*(v_c, t)$ and in the cold phase $m_c(v_c, t)$, as well as for the fraction f_* of ejected gas, the time increment of which is given by equation (6).

As for the X-ray luminosity, this is computed from the compression factor $G^2(M, M')$ (equation 2) inserted into equation (1). Its average value is computed by an analogous convolution to the above one:

$$L_X(v_c, t + \Delta t) = L_X(v_c, t) + \Delta t \int_0^{M(v_c)} \mathrm{d}M' \frac{N(M', t)}{N(M, t)} \frac{\partial^2 P(M', t|M)}{\partial M' \partial t} A \left(\frac{m_h}{M}\right)^2 G^2(M, M')\; T_v^2(M)\; \rho^{1/2}(z)\; I(M, t). \tag{8}$$

(iv) The values of m_c, m_* and m_h are reset for every v_c after all their (positive or negative) increments owing to cooling, SF, supernova feedback and merging have been computed in the steps (ii) and (iii).

(v) Finally, for each v_c the associated optical luminosity at the wavelength λ is computed by the convolution

$$S_\lambda = \int_0^t \phi_\lambda(t - t') m_*(t')\, \mathrm{d}t', \tag{9}$$

where the spectral energy distribution of luminous stars $\phi_\lambda(t)$ is taken from a canonical model of stellar population synthesis (Bruzual & Charlot 1993) in its latest version.

(vi) We increment the current time by Δt, and repeat the whole procedure through steps (ii) to (v) until the output time is reached.

We comment that our analytical rendition of the galaxy formation sector is technically similar to the formulation by White & Frenk (1991), but *differs* in a number of respects: (a) we consider here all three components (stars, cold gas phase, hot gas phase) which are involved in the SF process, while in the paper by White & Frenk (1991) only cold gas and stars where considered; (b) we implement the comprehensive recipe used in SAM for the star formation and feedback, while in White & Frenk (1991) a simplifying assumption of

Table 1. Model parameters. The parameters corresponding to the two reference SFRs introduced in the text. These define, as a function of the halo circular velocity v_c, the star formation timescale $\tau_*(v_c) = \tau_*^0(v_c/300\,\mathrm{km\,s^{-1}})^{\alpha_*}$ and the mass $\Delta m_h = (v_c/v_h)^{-\alpha_h}\Delta m_*(v_c, t)$ reheated by SN feedback.

	τ_*^o	α_*	v_h	α_h
Model A	2.8 Gyr	−1.5	140 km s^{-1}	5.5
Model B	2.8 Gyr	0	140 km s^{-1}	1.5

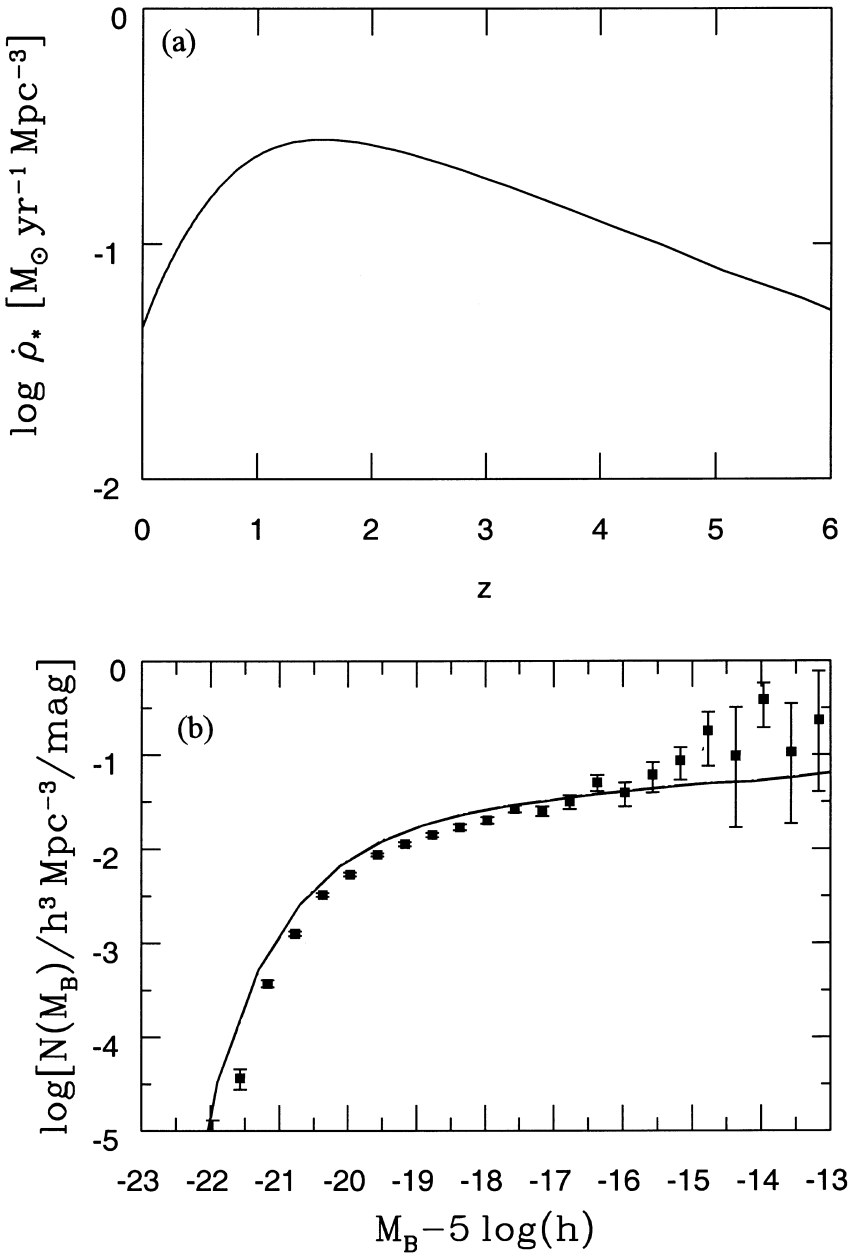

Figure 1. (a) The global star formation rate, as a function of redshift z for Model A. (b) The B-band luminosity function of galaxies for Model A; for comparison, we show the data by Zucca et al. (1997).

self-regulation had been adopted to obtain a simple expression for the SFR. On the other hand, we plan to add chemical enrichment models in an extension of this work.

Our main improvement concerns of course the insertion in the old framework of the novel issues concerning on the X-ray emitting baryons.

3 CHOICE OF PARAMETERS

In fact, our aim is to obtain the X-ray counterpart of different SF histories. We consider two *extreme* cases A and B, both consistent with the data discussed in the Introduction.

Model A is characterized by a SFR declining beyond $z \approx 2$, as was originally suggested by Madau et al. (1996), and as was obtained from the SAM (Baugh et al. 1998). From the latter authors, we adopt the set of parameters reproduced in the first row of our Table 1, and chosen by them to yield an acceptable fit to the local galaxy luminosity function. The resulting SFR we find (see Fig. 1a) is peaked at $z \approx 1.5$ and in fact declines considerably for $z \gtrsim 2$.

The corresponding galaxy luminosity function at $z = 0$ is shown in Fig. 1(b). As discussed by Cole et al. (1994, see their table 1; also

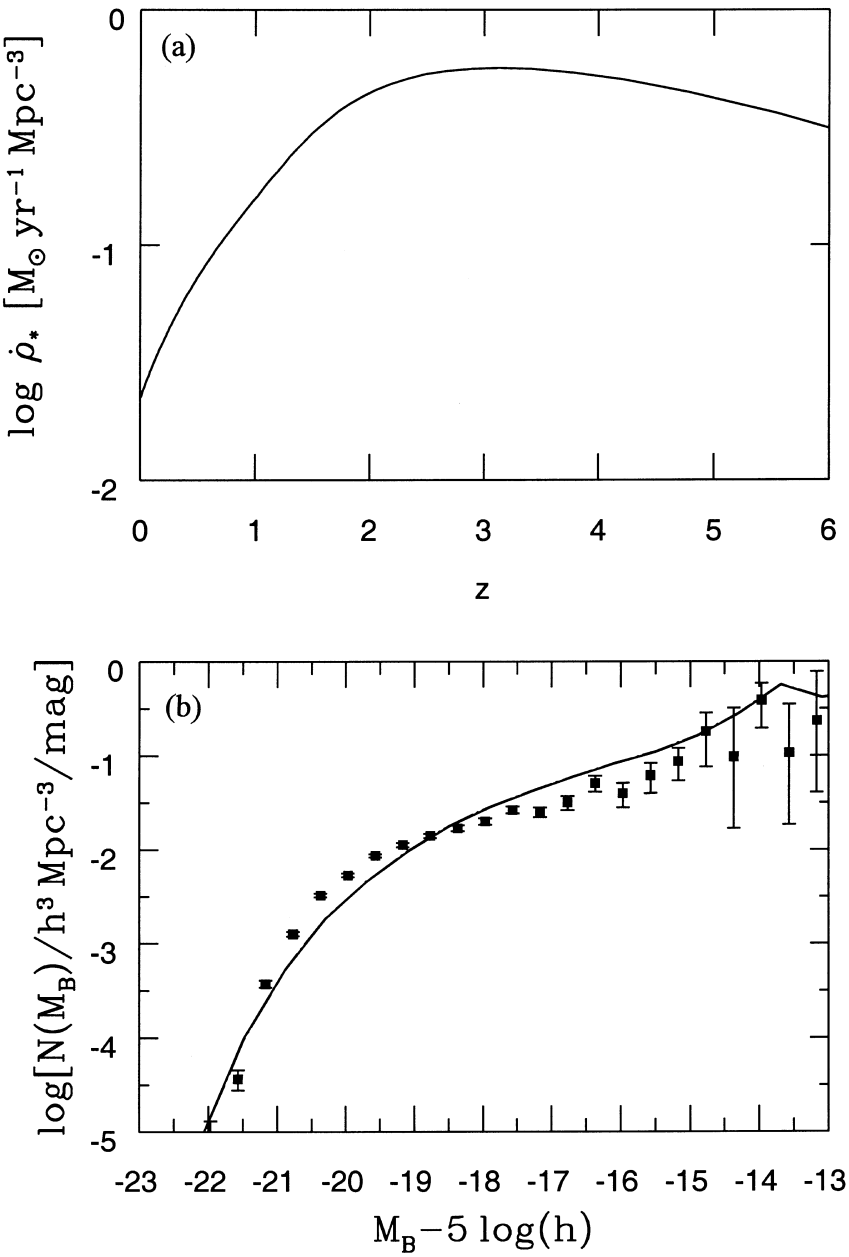

Figure 2. Same as Fig. 1, but from Model B.

Baugh et al. 1998), both the decline of the SFR at large z and the flat shape of the galaxy luminosity function are due to the strong supernovae feedback at small v_c resulting from their set of star formation and feedback parameters. The same feedback affects strongly the X-ray luminosities through the compression factor G^2 and the factor m_h^2 in equation (1).

Model B instead is characterized by a SFR flat beyond $z \approx 2$, see Fig. 2(a). The set of parameters leading to this are shown in the

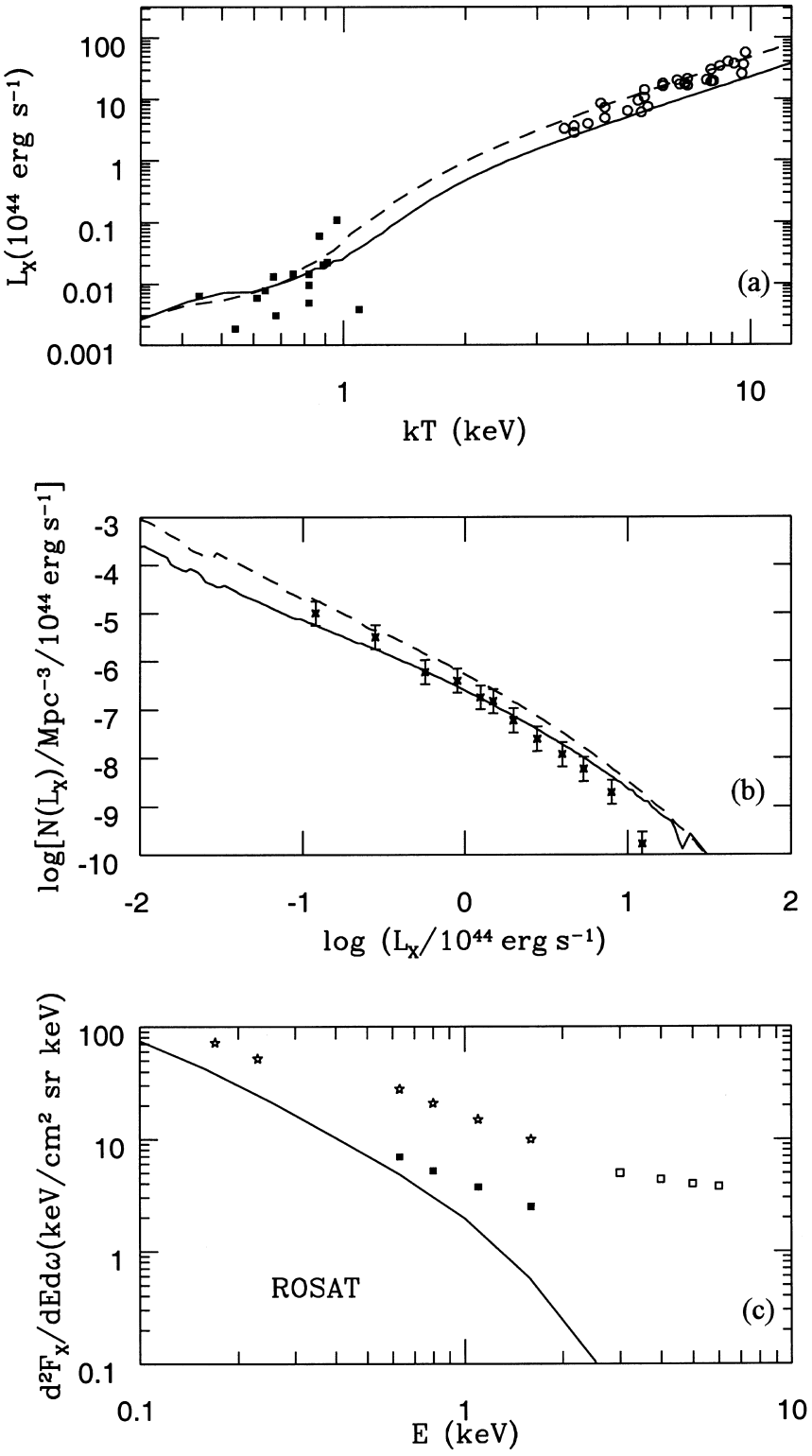

Figure 3. Results from Model A. (a) The $L_X - T$ correlation at $z = 0$ (solid line) and at z = 1 (dashed line). Group data from Ponman et al. (1996, solid squares); cluster data from Markevitch (1998, open triangles). (b) The local (solid line) and the $z = 1$ (dashed line) luminosity function. For comparison, we show the data by Ebeling et al. (1997). (c) The contribution of hot baryons to the soft X-ray background for sources with $F_X < 410^{-14}$ erg cm^{-2} s^{-1} is compared with the total observed values (open stars, Hasinger et al. 1998), and with the 25 per cent unresolved component (see Giommi et al. 1998, solid squares).

second row of Table 1. Such a choice corresponds to a milder feedback even in small haloes, consistent with recent works by Ferrara & Tolstoy (1999) and by Martin (1999). This yields a rather steep local galaxy luminosity function (Fig. 2b) below L_*, a feature considered tenable, if marginally, in view of the data by Zucca et al. (1997).

In deriving the galaxy luminosity functions we followed Cole et al. (1994) in normalizing the mass-to-light ratio in terms of Υ, the total mass in stars divided by the mass in luminous stars with mass $> 0.1\,M_\odot$. We adopted $\Upsilon = 2.7$ for Model A (the value of the fiducial model by Cole et al. 1994), and $\Upsilon = 2$ for Model B.

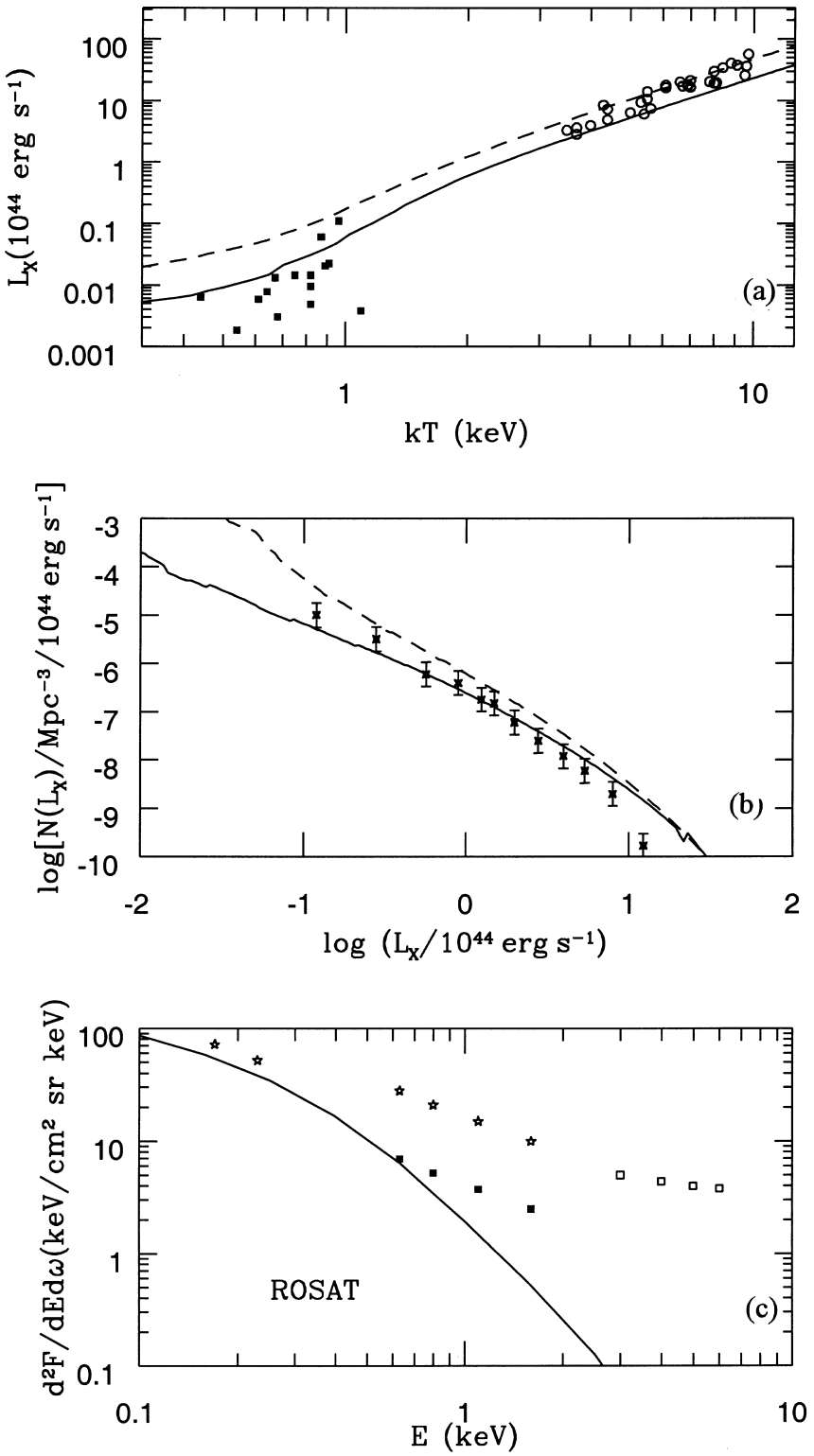

Figure 4. Same as Fig. 2, but for Model B.

For comparison with the SAMs, we adopt their 'fiducial' cosmological/cosmogonical context, namely the CDM model with $\sigma_8 = 0.67$, $\Omega = 1$, $\Omega_b = 0.06$ and $h = 0.5$. In all cases, the Scalo IMF has been adopted, as widely used in SAMs.

4 RESULTS

The outcomes in X-rays from Model A are shown in Fig. 3. The $L_X - T$ relation provides a good fit to the data (panel a) down to the sub-keV range, the region most affected by supernova feedback (equation 6). Note the mild evolution out to $z = 1$. The corresponding X-ray luminosity function (panel b) also agrees well with the local data (Ebeling et al. 1997; De Grandi et al. 1999) and shows little evolution out to $z \approx 1$ in agreement with recent data (Rosati et al. 1998). We also plot (panel c) the complementary contribution to the soft X-ray background (details are given in CMT98), which is well below the observational limits even when a 75 per cent resolved contribution is subtracted out of the *ROSAT* data (see Hasinger et al. 1998; Giommi, Fiore & Perri 1998).

The corresponding results for the opposite extreme Model B are shown in Fig. 4. Here the $L_X - T$ relation is flatter at low T, and constitutes a marginal fit to the existing data. This is because the lower amount of gas expelled by virtue of the smaller feedback (with a minor effect from the increased temperature T_*) reduces the changes with T of the compression factor G entering the X-ray luminosity (equation 1); the result is closer to the gravitational self-similar scaling $L \propto T_v^2$. This goes back to the circumstance (see Fig. 2) that, in the absence of an appreciable contribution $f_* g^2(T_*)$ from supernovae in the merging partner M', the prevailing term $(1 - f_*)g^2(T_v)$ is determined only by the virial temperature ratio $T_v(M)/T_v(M')$. Such ratio of purely gravitational temperatures does not change appreciably with T when averaged using the self-similar merging rates; so a nearly constant G^2 obtains, and equation (1) tends to $L \propto T_v^2$.

Another feature of Model B is the increase with z of the X-ray luminosities; this is a result of the larger amount of hot gas [the factor (m_h^2/M^2) in equation 1] made available by the stronger global, supernova activity, but retained in shallow wells by virtue of the weak feedback. This has a number of implications: not only the faster evolution of the $L_X - T$ relation represented by the dashed curve in panel (a), but also the increased number of faint sources represented in the luminosity functions $N(L,z)$ in panel (b); in addition, the contribution to the soft X-ray background is larger, and barely consistent with the observational limits.

However, the key X-ray test telling apart the two models is provided by the source counts $N(> F)$ shown in Fig. 5. The larger number of sources predicted at high z by model B implies faint counts larger by factors $\sim$4 relative to Model A; their redshift distributions are shown in Figs 6(a) and (b). Correspondingly, in Fig. 7 we show for the two models the luminosity density in X-rays, the counterpart for the hot baryons of the SFR associated with condensed baryons shown in Fig. 1. Note that for model B the peak is higher and shifted to $z \approx 2$, corresponding to the larger SF activity at high z. We also stress that, in any case, the effect of SF on the X-ray emission is always delayed by the few dynamical times taken by the merging activity (see equation 8) to affect the ICM.

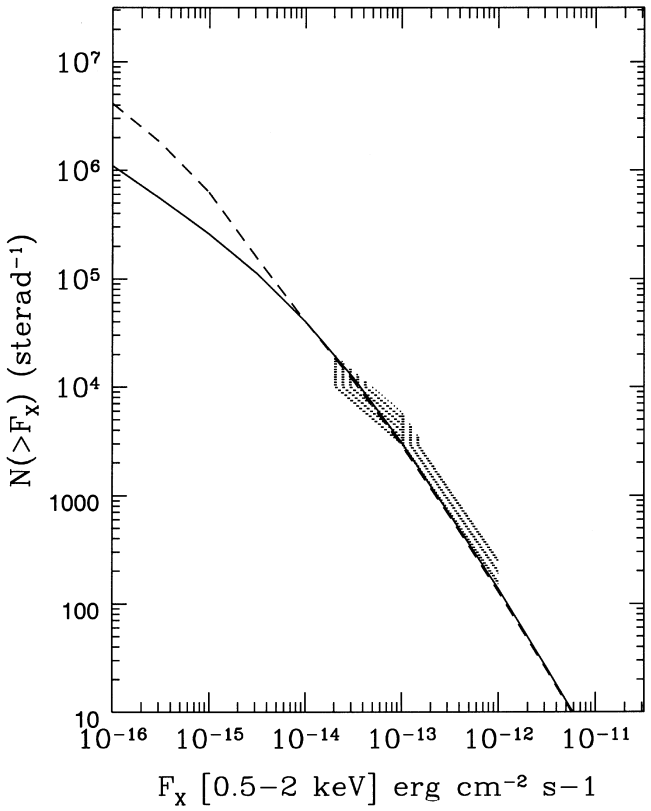

Figure 5. The source counts from Model A (solid line) and from Model B (dashed line), in the energy band 0.5–2 keV. The dashed region corresponds to the *ROSAT* cluster number counts observed by Rosati et al. (1998).

Finally, we show in Fig. 8 the correlation between the X-ray flux and the optical (B and K) magnitudes in DM haloes, as predicted by Model A and by Model B.

5 CONCLUSIONS

In this paper we have related two quantities: the X-ray emission from the hot diffuse baryons in hierarchically evolving potential wells, and the history of the baryons condensed into stars. We have presented a computational package that grafts on the extended Press & Schechter treatement of the hierarchical clustering both our model for the thermo- and the hydrodynamics of the X-ray emitting ICM, and our analytic implementation of the current recipes adopted in the semi-analytic models of galaxy formation.

We have shown that supernova feedback is an essential ingredient in deriving not only the early SFR, but also a realistic shape of the $L_X - T$ correlation for groups and clusters of galaxies, and in predicting counts and luminosity functions of faint X-ray sources. In fact, the SFR at $z \gtrsim 2$ depends strongly on the amount and the temperature of the baryons retained in *small* potential wells. But as such small haloes are included into larger structures at lower z, the same quantities affect the X-ray properties of the accreting haloes.

Specifically, we find that if the SFR is peaked at $z \approx 1.5$ with a *decline* to higher z, then the local $L_X - T$ correlation *flattens* strongly going from groups to rich clusters of galaxies, and evolves little with z; the corresponding luminosity density in X-rays is peaked at $z \simeq 1$. Conversely, if the SFR was already high since $z \approx 4$, then a *smoother* local $L_X - T$ relation would obtain, closer to the self-similar form $L_X \propto T^2$ down to poor groups. On a related note, the counts of such sources at fluxes brighter than $F_X \simeq 10^{-15}\,\mathrm{erg\,cm^{-2}\,s^{-1}}$ would exceed the former case by a factor 4 in the energy band $\gtrsim$0.5 keV. Even fainter fluxes are within the reach of the next generation X-ray observatories like *AXAF* or *XMM* (although near its confusion limit). To be conservative with surface brightness, we have included in the counts only $L_X \geqslant 10^{43}\,\mathrm{erg\,s^{-1}}$. In addition, the above excess counts has been computed with a conservative low-energy threshold (0.5 keV)

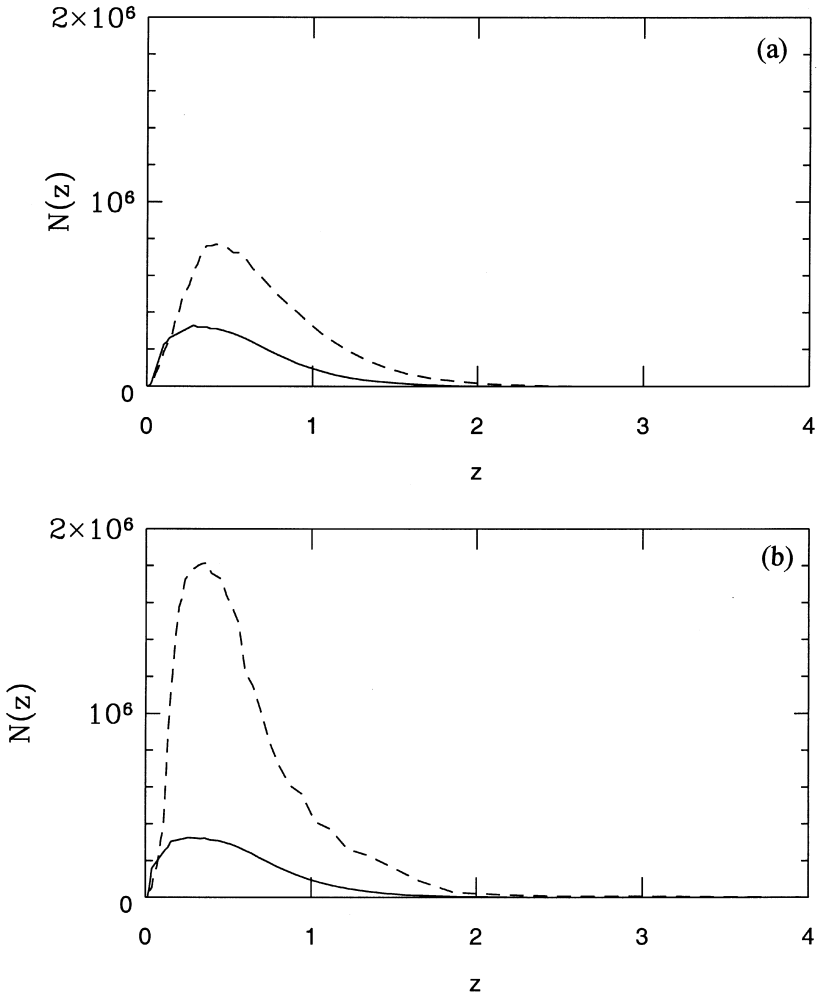

Figure 6. The redshift distribution of X-ray sources is plotted for different fluxes: $10^{-15} < F < 10^{-14}\,\mathrm{erg\,cm^{-2}\,s^{-1}}$ (solid line), and the very faint range $10^{-16} < F < 10^{-15}\,\mathrm{erg\,cm^{-2}\,s^{-1}}$ (dashed line). Panel (a) for Model A, panel (b) for Model B.

for *AXAF*, which in fact may have an effective threshold of 0.25 keV (R. Giacconi, private communication), while 0.1 keV is planned for *XMM*; for example, on lowering the threshold down to 0.25 keV the excess would be doubled.

All that will make in the near future the X-ray observations of groups and clusters a powerful means to probe the strength of the feedback processes, which determine also the SF history at high z. For example, the excess X-ray counts by a factor 4 corresponds to filling with stellar and hot baryons the early potential wells, to yield a SFR larger by $\sim$10 at $z \approx 3$–4.

We have investigated the sensitivity of our results to changes of the cosmological framework. We find that the difference between Model A and B persists when one considers different cosmologies within the usual constraints provided, e.g., by the cosmic age and the local counts of X-ray clusters. In particular, we have checked that for a flat Λ-cosmology ($\Omega_o = 0.3$, $\Omega_\lambda = 0.7$, $\Omega_b = 0.04$) the count excess is still larger than 3.5. A more extended study of the SFR-X-ray connection for different cosmologies will be presented elsewhere.

We have explored the effect of varying the star formation and feedback parameters, and of changing the star formation recipe altogether. We have first kept α_* fixed at 0, and tried values of α_h intermediate between Model A and B, yielding intermediate decline of the SFR at $z \gtrsim 2$. We find X-ray counts again exceeding those of Model A for any value of $2 \leqslant \alpha_h < 5.5$; e.g., at $F_X = 10^{-15}$ erg cm^{-2} s^{-1} for $\alpha_h = 3.5$ the excess over Model A is a factor 2.3, while for $\alpha_h = 4$ the excess is still factor 1.9; recall that when the energy band is extended down to 0.25 keV the difference between this case and Model A is doubled. Thus, soft X-ray observations, as planned for the next space observatories can pinpoint the effective strength of the feedback within the range defined by our extreme Models A and B. If we now change α_* to the other extreme value -1.5, the above results are not changed appreciably. This is because it is the feedback which dominates (see Cole et al. 1994) the amount and the thermal state of all baryons in shallow, early potential wells, and so governs both the X-ray emission and the SFR at large values of z.

We have also investigated the effect of adopting recipes for the star formation and for the feedback different from Cole et al. (1994). In particular, we implemented in detail the recipe by Kauffmann et al. (1993), where all the gas is retained in the haloes and the feedback parameter has about the same v_c-dependence of our Model B. This yields a flat SFR at $z > 2$; but in addition we obtain X-ray counts close to those in Model B, confirming the trend: more stars – more X-rays. However, the lower normalization of the feedback leads in this case to a very flat local $L_X - T$ correlation.

Finally, we have checked that our results are little sensitive to the inclusion of additional, reasonable heating or cooling. Specifically,

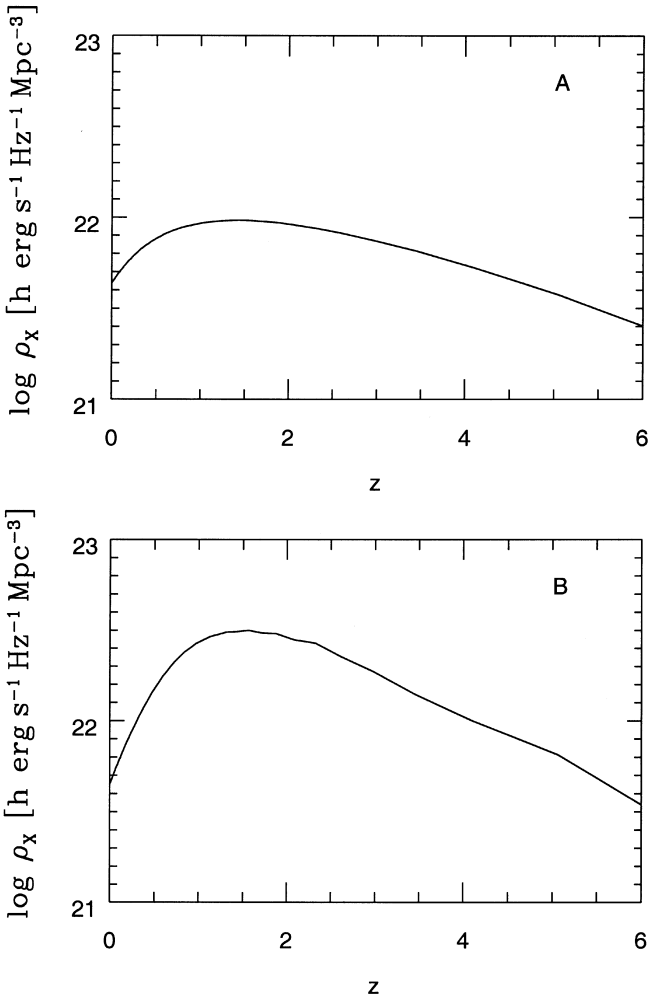

Figure 7. The X-ray luminosity density (for photon energies in the range 0.1–10 keV) as a function of redshift. Panel (a) Model A, panel (b) Model B. These constitute the X-ray counterparts of the O–UV luminosity density corresponding to the SFR shown in Fig. 1

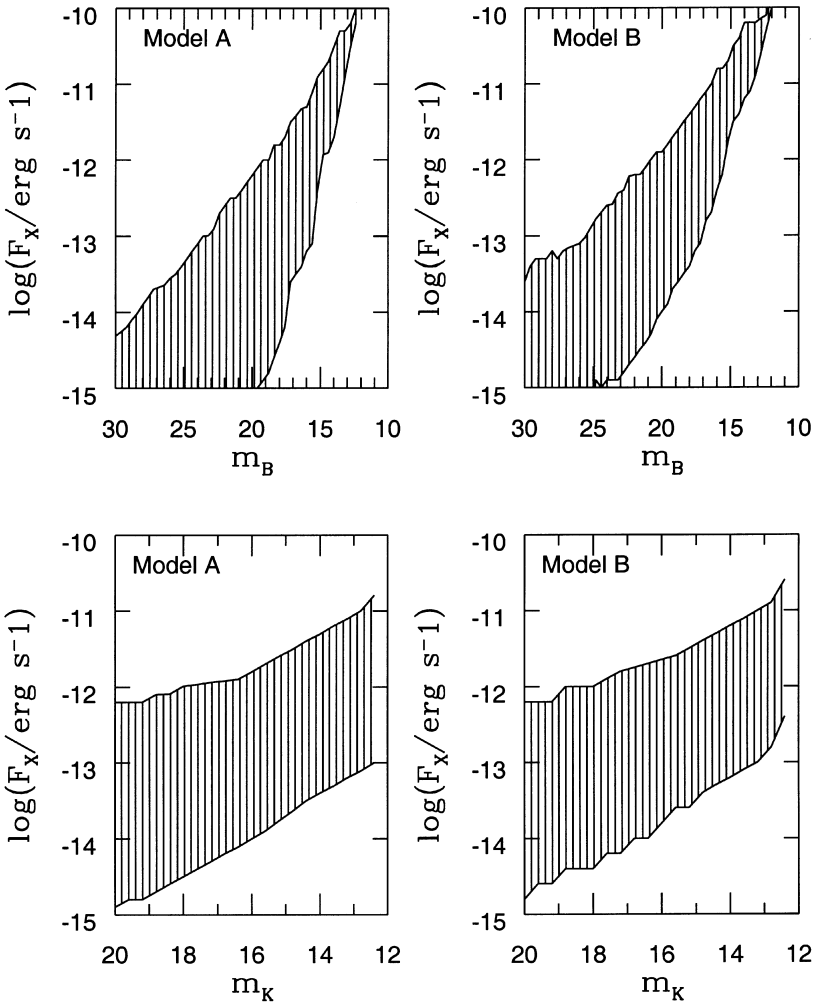

Figure 8. The correlation between X-ray fluxes and optical magnitudes is plotted (shaded region) for *B* magnitudes (upper two panels) and *K* magnitudes (lower two panels), for Model A (left column) and Model B (right column)

the supernova heating inside the deep wells turns out to be not relevant, unless the associated T_* is forced up to values close to the virial temperature around 10 keV, at variance with the accepted star and supernova energetics. Such findings are consistent with those by Metzler & Evrard (1997) based on hydrodynamical/*N*-body simulations. On the other hand, considering explicitly the cooling of the gas ejected beyond the virial *R*, the temperature T_* decreases by only 5–10 per cent, owing to the low densities of the gas in the external regions. This holds both for a distribution spread outside *R* with a density following the DMs, and for a constant density shell of thickness $v_{\rm esc}\Delta t$ located at *R*.

In summary, the thermal state and amount of hot baryons (with their X-ray emission) and of the condensed baryons in shallow potential wells (yielding the SFR at high z observed in the O–UV bands) both depend on the same energy feedback from supernovae. The X-ray and the O–UV bands concur to yield predictions and information concerning the baryon history; in particular, the X-rays catch *directly* the feedback in the act and probe its effective strength. We add that, while in this paper we have focussed on the truly hot component (at $T \sim 10^6$–10^8 K, making up a minor but vocal fraction of all baryons), the connection here investigated involves other baryonic phases, observable in different bands; e.g., the lukewarm ($T < 5\,10^4$ K) gas contributing to the the different SF histories can be compared with the amount of photoionized gas probed by absorbtion in the Ly-α clouds (both in and out the galaxies). Such a variety of independent probes will tightly bound the amount and behaviour of the feedback processes; these are presently highly uncertain, but in fact govern the early cosmic SFR and so the emission properties of the faint galaxy population.

ACKNOWLEDGMENTS

This work has been triggered by a discussion with R. Giacconi who posed the question of any connection between the planned *AXAF* deep counts and the optical SFR. Informative discussions with P. Rosati are also gratefully acknowledged. We thank our referee for stimulating and helpful comments.

REFERENCES

Allen S. M., Fabian A. C., 1998, MNRAS, 297, L57
Balogh M. L., Babul A., Patton D. R., 1998, preprint (astro-ph/9809159)
Barger A., Cowie L. L., Sanders D. B., Fulton E., 1999, Nat, 394, 248
Baugh C. M., Cole S., Frenk C. S., Lacey C. G., 1998, ApJ, 498, 504
Bond J. R., Cole S., Efstathiou G., Kaiser N., 1991, ApJ, 379, 440
Bower R., 1991, MNRAS, 248, 332
Bruzual A. G., Charlot S., 1993, ApJ, 405, 538
Cavaliere A., Menci N., Tozzi P., 1997, ApJ, 484, L1 (CMT97)
Cavaliere A., Menci N., Tozzi P., 1998, ApJ, 501, 493 (CMT98)
Cavaliere A., Menci N., Tozzi P., 1999, MNRAS, 308, 599 (CMJ99)
Cole S., Aragon-Salamanca A., Frenk C. S., Navarro J. F., Zepf S. E., 1994, MNRAS, 271, 781
Connolly A. J., Szalay A. S., Dickinson M. E., Subbarao M. U., Brummer R. J., 1997, ApJ, 486, L11
De Grandi S. et al., 1999, ApJ, 513, 17
Dickinson M., 1997, in Livio M. et al., eds, *Hubble* Deep Field. Cambridge Univ. Press, Cambridge, p. 219
Ebeling H., Edge A. C., Fabian A. C., Allen S. W., Crawford C. S., Böhringer H., 1997, preprint (astro-ph/9701179)
Edge A. C., Stewart G. C., 1991, MNRAS, 252, 428
Ellis R., 1998, Nat, 395, 3
Ferrara A., Tolstoy E., 1999, preprint (astro-ph/9905280)
Fukugita M., Hogan C. J., Peebles P. J. E., 1998, ApJ, 479, 101
Giommi P., Fiore F., Perri M., 1998, preprint (astro-ph/9812305)
Hasinger G., 1996, A&AS, 120, 607
Hasinger G. et al., 1998, A&A, 329, 482
Hughes D. et al., 1998, Nat, 394, 241
Kaiser N., 1986, MNRAS, 222, 323
Kauffmann G., White S. D. M., Guiderdoni B., 1993, MNRAS, 264, 201
Lacey C., Cole S., 1993, MNRAS, 262, 627
Madau P., Ferguson H. C., Dickinson M. E., Giavalisco M., Steidel C. C., Fruchter A., 1996, MNRAS, 283, 1388
Madau P., Pozzetti L., Dickinson M. E., 1998, ApJ, 498, 106
Markevitch M., 1998, ApJ, 504, 27
Martin C. L., 1999, ApJ, 513, 156
Metzler C. A., Evrard A. E., 1997, preprint (astro-ph/9710324)
Meurer G., Heckman T. M., Lehnert M. D., Leitherer C., Lowenthal J., 1997, AJ, 111, 54
Navarro J. F., Frenk C. S., White S. D. M., 1997, ApJ, 490, 493
Peebles P. J. E., 1993, Principles of Physical Cosmology. Princeton Univ. Press, Princeton
Pettini M. et al., 1997, in Waller W. et al., eds, AIP Conf. Proc. 408, The Ultraviolet Universe at Low and High Redshift: Probing the Process of Galaxy Evolution. Am. Inst. Phys., New York, p. 279
Poli F., Giallongo E., Menci N., Cristiani S., D'Odorico S., 1999, preprint
Ponman T. J., Bourner P. D. J., Ebeling H., Böhringer H., 1996, MNRAS, 283, 690
Ponman T. J., Cannon D. B., Navarro J. F., 1999, Nat, 397, 135
Press W. H., Schechter P., 1974, ApJ, 187, 425
Rosati P., Della Ceca R., Norman C., Giacconi R., 1998, ApJ, 492, 21
Smail I., Ivison R. G., Blain A. W., 1997, ApJ, 490, L5
Somerville R. S., Primack J. R., 1998, preprint (astro-ph/9802269)
Steidel C. C., Adelberger K. L., Giavalisco M., Dickinson M., Pettini M., 1999, ApJ, 519, 1
White D. A., Fabian A. C., 1995, MNRAS, 273, 72
White S. D. M., Navarro J. F., Frenk C. S., Evrard A. E., 1993, Nat, 366, 429
White S. D. M., Frenk C. S., 1991, ApJ, 379, 52
Zucca E. et al., 1997, A&A, 326, 477

This paper has been typeset from a TEX/LATEX file prepared by the author.